Nagarkar et al. International Journal of Mechanical and Materials Engineering (2018) 13:10
https://doi.org/10.1186/s40712-018-0096-8

International Journal of Mechanical and Materials Engineering

ORIGINAL PAPER Open Access

GA-based multi-objective optimization of active nonlinear quarter car suspension system—PID and fuzzy logic control

Mahesh P. Nagarkar[1,2*], Yogesh J. Bhalerao[3], Gahininath J. Vikhe Patil[2] and Rahul N. Zaware Patil[4]

Abstract

Background: The primary function of a suspension system is to isolate the vehicle body from road irregularities thus providing the ride comfort and to support the vehicle and provide stability. The suspension system has to perform conflicting requirements; hence, a passive suspension system is replaced by the active suspension system which can supply force to the system. Active suspension supplies energy to respond dynamically and achieve relative motion between body and wheel and thus improves the performance of suspension system.

Methods: This study presents modelling and control optimization of a nonlinear quarter car suspension system. A mathematical model of nonlinear quarter car is developed and simulated for control and optimization in Matlab/Simulink® environment. Class C road is selected as input road condition with the vehicle traveling at 80 kmph. Active control of the suspension system is achieved using FLC and PID control actions. Instead of guessing and or trial and error method, genetic algorithm (GA)-based optimization algorithm is implemented to tune PID parameters and FLC membership functions' range and scaling factors. The optimization function is modeled as a multi-objective problem comprising of frequency weighted RMS seat acceleration, Vibration dose value (VDV), RMS suspension space, and RMS tyre deflection. ISO 2631-1 standard is adopted to assess the ride and health criterion.

Results: The nonlinear quarter model along with the controller is modeled and simulated and optimized in a Matlab/Simulink environment. It is observed that GA-optimized FLC gives better control as compared to PID and passive suspension system. Further simulations are validated on suspension system with seat and human model. Parameters under observation are frequency-weighted RMS head acceleration, VDV at the head, crest factor, and amplitude ratios at the head and upper torso (AR_h and AR_ut). Simulation results are presented in time and frequency domain.

Conclusion: Simulation results show that GA-based FLC and PID controller gives better ride comfort and health criterion by reducing RMS head acceleration, VDV at the head, CF, and AR_h and AR_ut over passive suspension system.

Keywords: Multi-objective optimization, Genetic algorithm, Nonlinear quarter car, PID, FLC

* Correspondence: maheshnagarkar@rediffmail.com
[1]SCSM College of Engineering, Ahmednagar, MS 414005, India
[2]Research Department of Mechanical Engineering, AVCoE, Sangamner, MS, India
Full list of author information is available at the end of the article

Springer Open

© The Author(s). 2018 **Open Access** This article is distributed under the terms of the Creative Commons Attribution 4.0 International License (http://creativecommons.org/licenses/by/4.0/), which permits unrestricted use, distribution, and reproduction in any medium, provided you give appropriate credit to the original author(s) and the source, provide a link to the Creative Commons license, and indicate if changes were made.

Background

The main function of an automotive suspension system is to support the vehicle weight, to isolate the occupants against the excitations caused by road unevenness and thus providing the ride comfort and better handling, and to keep the contact between tyre and ground. The task of the suspension system is a trade-off between ride and performance as ride comfort needs soft suspension system whereas to follow track and support vehicle weight stiff suspension system is required.

The primary objective of the active suspension system is to replace the passive suspension system by a controlled system which can supply force to the system. Active suspension supplies energy to respond dynamically and achieve relative motion between the body and the wheel. Thus, to changing road conditions, active suspension system improves the performance of the suspension system such as ride comfort, suspension or rattle space displacement, tyre displacement, and body displacements (Wong 2001). For active control, various control strategies are implemented like optimal control, robust control, nonlinear control, nonlinear control with backstepping, sliding mode control, intelligent control, neural control, and hybrid control. One of the main objectives was to minimize body acceleration to improve ride comfort.

Metered et al. (2015) had implemented particle swarm optimization (PSO) algorithm to tune the PID controller implemented on a semi-active quarter car suspension system. A 2DoF model with MR damper is simulated in a Matlab/Simulink environment with bump and random road inputs. The system was tested in time and frequency domain. It was observed that POS tuned PID controller improves ride comfort and vehicle stability. Kesarkar and Selvaganesan (2015) designed fractional order PID controller using artificial bee colony algorithm with objective functions such as integral absolute error, integral square error, and integral time absolute error implemented to a multi-modal complex optimization problem. The authors observed that the results were promising as compared to the conventional PID method. Niu (2014) had implemented GA-based optimization method to tune PID parameters of the active suspension system. Absolute error control is used as an objective function to tune the PID parameters. It was observed that the GA-based optimized PID controller improves the dynamic performance of the active suspension system and improves stability. Gad et al. (2017) implemented a fractional order PID controller to a semi-active seat suspension. PID parameters are tuned using multi-objective GA for a seat suspension system using the 6-DoF human body. It is observed that GA-based PID controller improved SEAT value, VDV ratio, and crest factor as compared to the passive system and classical PID controller. Results are obtained in time as well as frequency domain. Tammam et al. (2013) implemented a multi-objective GA-based PID controller to control the load frequency of a single area power system. It is observed that GA-based PID controller is simple and easy to implement and improves system performance effectively. Abdelrassoul et al. (2016) studied the performance of the PV system based on GA-optimized PID controller. Here, PID controller is implemented to enhance PV system output with minimum overshoot and minimum rise time in output voltage with the better response. Chen and Chang (2006) studied GA-based PID tuning for active magnetic bearing. The proposed PID controller shows that the active magnetic bearing had good static and dynamic performance and showed better performance and effectiveness.

It is observed that optimization of PID controller applied to suspension system is carried out in single objective nature (Metered et al. 2015; Niu 2014) whereas (Kesarkar and Selvaganesan 2015) presented a multi-modal optimization approach and (Gad et al. 2017) presented dual objective function optimization.

Kalaivani et al. (2014) studied a fuzzy logic-based active quarter car suspension system. A hybrid differential evolution bio-geography based optimization algorithm is used to tune the FLC controller. RMS body acceleration is used as performance index to study the PID and newly proposed FLC controller. It was observed that the proposed controller improves the ride comfort. Taskin et al. (2017) implemented the FLC controller on a quarter car test rig. Time and frequency domain response of sprung mass displacement, acceleration, and suspension space deflection and actuator force are studied and compared with passive suspension system and observed that FLC controller performance better. Huang and Chao (2000) implemented a fuzzy logic controller-based active suspension system on a quarter car model. Results showed that the control strategy improves ride comfort reducing the oscillations of the body. Salem and Aly (2009) had studied the 2-DoF quarter suspension system. FLC is used to control the quarter car active suspension system. Body acceleration is used as a criterion to study the ride comfort of a suspension system, along with handling. FLC and PID controller are studied and observed that FLC performs better compared to the PID controller. Rajendiran and Lakshmi (2016) analyzed active control of 2-DoF suspension system using PID control and FLC along with seat and driver model. It was observed that FLC improves ride comfort than that of PID control and passive system. Taskin et al. (2007) studied the FLC controller to enhance ride comfort. From time response of the active system, it is observed that body displacement is minimized without losing suspension working space. Results were obtained in the frequency domain which shows improved ride comfort. From above discussions, it is observed that researchers (Taskin et al. 2017; Huang

and Chao 2000; Salem and Aly 2009; Rajendiran and Lakshmi 2016) have successfully implemented the FLC for ride control applications, whereas (Kalaivani et al. 2014) optimized FLC using a single optimization function.

Talib and Darus (2014) implemented a semi-active suspension system using FLC and PID controllers. Performance of both the controllers is optimized by the PSO algorithm for mean square error. Optimized FLC, PID controllers are compared with a passive suspension system for body displacement, acceleration, tyre displacement for bump, and hole disturbances. It is observed that the FLC controller gave better results as compared to the PID controller. Celin and Rajeswari (2012) implemented type-2 FLC to the active suspension system. Sprung mass displacement, RMS acceleration, suspension space, and tyre deflection criterions were used to study the FLC and passive suspension system. GA-coded FLC outperforms the FLC and passive suspension system. D'Amato and Viassolo (2000) presented the active suspension system to reduce the body acceleration to improve comfort. FLC is used to control where parameters are tuned by GA optimization. This methodology improves ride comfort thus was effective in case of a quarter car suspension system. Li and Du (2006) presented a GA-based approach to optimize rule base and scaling factors. The parameters were coded into real-coded strings and treated as chromosomes during optimization. The GA-based optimization approach improves the performance of FLC. Liu et al. (2016) had successfully optimized the membership functions of FLC to a maximum power point tracking (MPPT) algorithm using PSO algorithm to improve averaged tracking error and fitness value. Bouarroudj et al. (2017) had presented the comparative analysis of Mamdani FLC with Gaussian membership functions for MPPT of PV system using GA and PSO approach. It was observed that PSO and GA optimized FLC gives better results in terms of performance.

This paper presents the mathematical modelling of a nonlinear quarter car (NLQC) along with a human model. The nonlinear quarter car model consists of quadratic tyre stiffness and cubic stiffness in suspension spring as nonlinearities. PID and FLC are implemented with the control objective to minimize frequency weighted RMS sprung mass acceleration (hereafter called as RMS sprung mass acceleration), VDV, RMS suspension space requirement, and RMS tyre deflection along with RMS optimal control force. The constraints on optimization are maximum control force, maximum sprung mass acceleration, maximum suspension space requirement, and maximum tyre deflection. Due to multi-objective natures of optimal control and conflicting control objectives, the key issue is to select the PID gain values and range of fuzzy input and output membership functions and scaling factors to fulfill the conflicting requirements. Trial and error method and or manual tuning of the PID controller and FLC are cumbersome and time-consuming. Hence, a GA-based evolutionary optimization technique is used to search the optimum parameters. During optimization, a nonlinear optimal control system is simulated in a Matlab/Simulink® environment where the tuning parameters are selected from the search space. The output of the nonlinear optimal control system is fed to the optimization algorithm to determine the objectives and validate the constraints. The optimization procedure is repeated up to 100 generations. Further, the optimization results are validated on a quarter car with seat and human model. Results are presented in both time domain and frequency domain.

Methods

Mathematical modelling—nonlinear quarter car suspension-seat-human model

A suspension system consists of damper and coil springs. Researchers have used various mathematical models viz. quarter car model having 2-DoF, a half car model having 4-DoF, and full car model. In this study, a 2-DoF quarter-car model is implemented for ride and control applications (Metered et al. 2015; Kalaivani et al. 2014; Taskin et al. 2017; Huang and Chao (2000); Salem and Aly 2009; Rajendiran and Lakshmi 2016).

Mathematical modeling is carried out using linear springs and damper by various authors (Kalaivani et al. 2014; Taskin et al. 2017; Huang and Chao (2000); Salem and Aly 2009; Rajendiran and Lakshmi 2016). But it is observed that spring exhibits nonlinear nature so do the tyre (Fuller et al. 1996). Thus, the nonlinearity should be considered during modeling. McGee et al. (2005) studied nonlinearities in the suspension system using a frequency domain technique and are validated experimentally with shaker data. It was observed quadratic and cubic stiffness and Coulomb friction nonlinearities in the suspension system (McGee et al. 2005). A chaotic response was presented by Zhu and Ishitobi (2006). They used a 7-DoF model with tyre stiffness and suspension spring stiffness nonlinearities. Bifurcation and chaotic response of 2-DoF model with tyre stiffness and suspension spring stiffness nonlinearities were presented by Lixia and Wanxiang (2008).

In the present analysis, a nonlinear quarter car model having quadratic tyre stiffness and cubic stiffness in suspension spring nonlinearities are considered.

A human model suggested by (Boileau and Rakheja 1998) is incorporated further in this study. The model is having 4-DoFs consisting of head and neck mass (m_h), chest and upper torso mass (m_{ut}), lower torso mass (m_{lt}), and thigh and pelvis mass (m_t). The human model considers typical driving conditions such as seated posture with feet support and hands held in driving conditions (refer to Fig. 1).

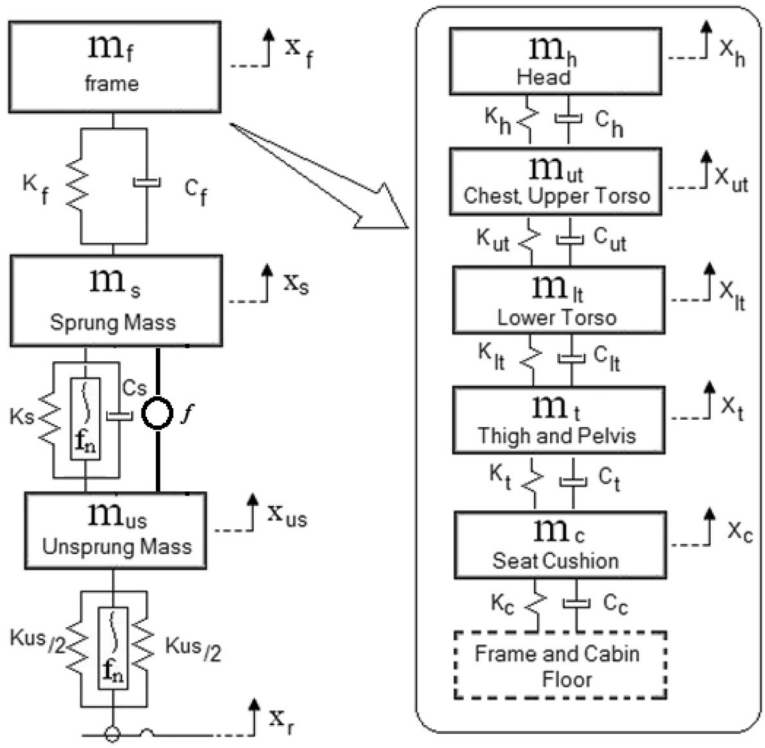

Fig. 1 Nonlinear quarter car suspension system—with seat and human model (Nagarkar et al. 2016)

According to D'Alembert's principle, the governing equations of motion representing nonlinear quarter car suspension-seat-human model are represented as –

$$
\begin{aligned}
m_{us}\ddot{x}_{us} &= -k_t(x_{us}-x_r) + k_s(x_s-x_{us}) + c_s(\dot{x}_s-\dot{x}_{us}) + k_{tnl}(x_{us}-x_r)^2 \\
&\quad +k_{snl}(x_s-x_{us})^3 - f \\
m_s\ddot{x}_s &= -k_s(x_s-x_{us}) - c_s(\dot{x}_s-\dot{x}_{us}) - k_{snl}(x_s-x_{us})^3 + k_f(x_f-x_s) \\
&\quad +c_f(\dot{x}_f-\dot{x}_s) + f \\
m_f\ddot{x}_f &= -k_f(x_f-x_s) - c_f(\dot{x}_f-\dot{x}_s) + k_c(x_c-x_f) + c_c(\dot{x}_c-\dot{x}_f) \\
m_c\ddot{x}_c &= -k_c(x_c-x_f) - c_c(\dot{x}_c-\dot{x}_f) + k_{tp}(x_t-x_c) + c_{tp}(\dot{x}_t-\dot{x}_c) \\
m_t\ddot{x}_t &= -k_{tp}(x_t-x_c) - c_{tp}(\dot{x}_t-\dot{x}_c) + k_{lt}(x_{lt}-x_t) + c_{lt}(\dot{x}_{lt}-\dot{x}_t) \\
m_{lt}\ddot{x}_{lt} &= -k_{lt}(x_{lt}-x_t) - c_{lt}(\dot{x}_{lt}-\dot{x}_t) + k_{ut}(x_{ut}-x_{lt}) + c_{ut}(\dot{x}_{ut}-\dot{x}_{lt}) \\
m_{ut}\ddot{x}_{ut} &= -k_{ut}(x_{ut}-x_{lt}) - c_{ut}(\dot{x}_{ut}-\dot{x}_{lt}) + k_h(x_h-x_{ut}) + c_h(\dot{x}_h-\dot{x}_{ut}) \\
m_h\ddot{x}_h &= -k_h(x_h-x_{ut}) - c_h(\dot{x}_h-\dot{x}_{ut})
\end{aligned}
\tag{1}
$$

The nonlinear quarter car seat-suspension-human model parameters are as follows:

$m_h = 5.31$; $c_h = 400$; $k_h = 310{,}000$;
$m_{ut} = 28.49$; $c_{ut} = 4750$; $k_h = 183{,}000$;
$m_{lt} = 8.62$; $c_{lt} = 4585$; $k_{lt} = 162{,}800$;
$m_t = 12.78$; $c_t = 2064$; $k_t = 90{,}000$;
$m_c = 1$; $c_c = 200$; $k_c = 18{,}000$;
$m_f = 15$; $c_f = 830$; $k_f = 31{,}000$;
$m_s = 290$; $c_s = 700$; $k_s = 23{,}500$; $k_{snl} = 100k_s$ (Lixia and Wanxiang 2008);
$m_{us} = 40$; $k_t = 190{,}000$; $k_{tnl} = 1.5\ k_t$ (Zhu and Ishitobi 2006).

The nonlinear quarter car having quadratic stiffness nonlinearity in the tyre and cubic stiffness in suspension spring is modeled and simulated in Matlab/Simulink®. Further, the simulations are carried out on a quarter car model with seat consisting frame and cushion with a human model.

Control theory—PID control

PID stands for proportional, integral, and derivative and is a classical controller used for several control applications (Metered et al. 2015; Kesarkar and Selvaganesan 2015; Niu 2014; Gad et al. 2017; Tammam et al. 2013; Abdelrassoul et al. 2016; Chen and Chang 2006). The PID controllers are so designed that continuous attention of the operator is eliminated. As the PID controller has designed a derivative nature type, small variation of output can be easily avoided. A PID controller is depicted in Fig. 2. The set point is where the

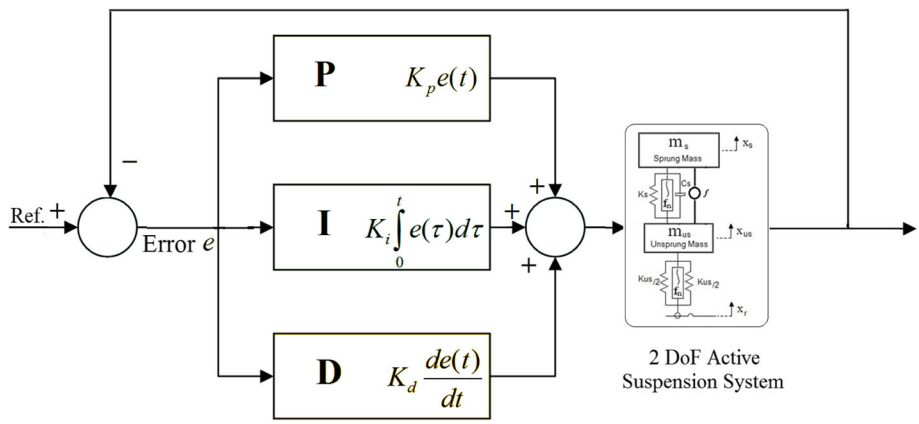

Fig. 2 PID control

measurement should be. An error is defined as the difference between the set point $r(t)$ and measurement $y(t)$. PID computes the control signal based on the following equations:

$$u(t) = K_p\, e(t) + K_i \int e(t)dt + K_d\, \frac{d}{dt} e(t) \tag{2}$$

$$e(t) = r(t) - y(t) \tag{3}$$

The error, e(t), variable being adjusted is called the manipulated variable which usually is equal to the output of the controller. As there is a change in measurement or set point, so is the output of the controller. Generally, Z-N tuning or auto-tuning is used to tune the P, I and D parameters of the controller.

Control theory—fuzzy logic control

FLC uses heuristic information for control applications. The FLC uses rule-base derived through an operator's experience and thus acts as a human-in-the-loop controller providing human experience to achieve high performance (Kalaivani et al. 2014; Taskin et al. 2017; Huang and Chao 2000).

Figure 3 represents the structure of a typical FLC implemented for a 2-DOF suspension system. Here, two inputs (error e and ec) and one output (force f_{FLC}) FLC with rule-base is implemented. Sprung mass velocity (error e) and acceleration (change in error ec) are used as input, and control force (f_{FLC}) is output. FLC rule base is a linguistic-based rule base which incorporates past human experience. Table 1 represents the rule base for two input-one output rule base for ride comfort. Figure 4 represents the surface plot rule base as stated in Table 1.

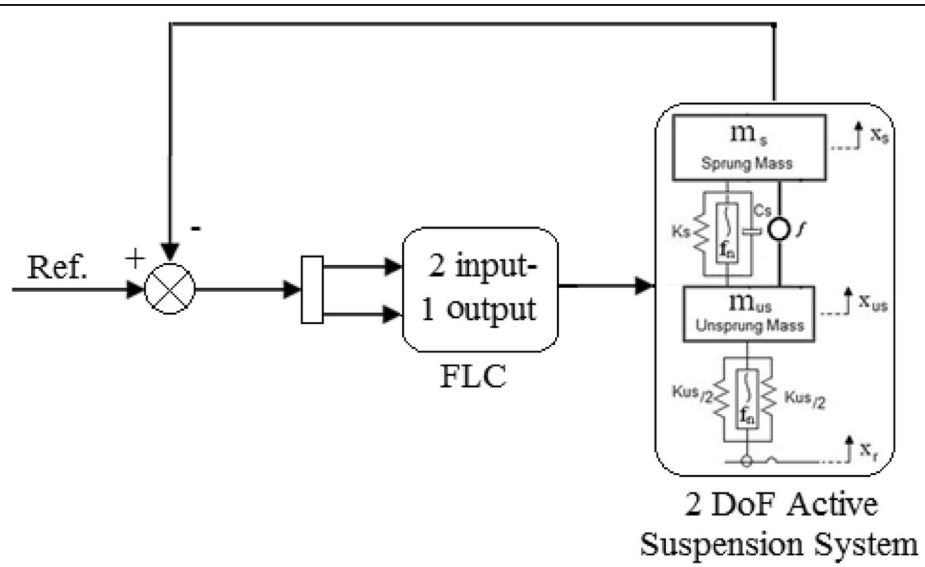

Fig. 3 Fuzzy logic controller

Table 1 Fuzzy logic rule table (2-DoF active suspension system)

f	ec							
e		NL	NM	NS	ZE	PS	PM	PL
	NL	PL	PL	PM	PS	PS	PS	ZE
	NM	PL	PM	PS	PS	PS	ZE	NS
	NS	PM	PS	ZE	ZE	ZE	NS	NM
	ZE	PM	PS	ZE	ZE	ZE	NS	NM
	PS	PM	PS	ZE	ZE	ZE	NS	NM
	PM	PS	ZE	ZE	ZE	ZE	NM	NL
	PL	ZE	NS	NS	NS	NM	NL	NL

N negative, *ZE* zero, *P* positive, *L* large, *M* medium, *S* small

Firstly, FLC decomposes the input into fuzzy sets, called as fuzzification, using membership functions (MF). Primarily membership functions map practical space to fuzzy space, known as fuzzification. Here, trapezoidal membership functions are used for input and output variables (refer Figs. 5, 6, and 7). The FLC consists of seven membership functions each, ie., for two inputs (error e and change in error ec) and an output f_{FLC}; these are NL, NM, NS, ZE, PS, PM, PL. Mamdani type fuzzy inference system (FIS) is used. Defuzzification is the process which maps the variables back to practical space from fuzzy space. Centroid defuzzification method is used in this FLC.

Objective functions

One of the key factors in optimization problems is to choose proper objective functions. Here, the control strategies are implemented to improve ride characterized by RMS sprung mass acceleration, VDV, RMS suspension space deflection, RMS tyre deflection, and RMS controller force.

RMS acceleration

As per ISO 2631-1 (1997), RMS acceleration is given by

$$A_{\mathrm{ws}} = \{\frac{1}{\mathrm{T}}\int_0^{\mathrm{T}}[\mathrm{a_w}(t)]^2\mathrm{dt}\}^{\frac{1}{2}} \tag{4}$$

A major portion of the vibration experienced by the occupants of an automobile enters the body through the seat (Van Niekerk et al. 2003; Bovenzi 2005). The health risk increases as the exposure time to vibrations increases. Hence, is it necessary to measure the whole body vibrations for ride and health criterion. As per ISO 2631-1 (1997), VDV is one measure for whole body vibrations. VDV also called as fourth power vibration dose. VDV is the method of assessing the cumulative effect (dose) of the vibration.

Vibration dose value (VDV)

VDV is the fourth power of acceleration time histories. It is expressed as -

$$\mathrm{VDVs} = \left\{\int_0^{\mathrm{T}}[\mathrm{a_w}(t)]^4\mathrm{dt}\right\}^{\frac{1}{4}} \tag{5}$$

Suspension travel

Suspension travel is characterized by the relative travel between the sprung mass and unsprung mass. Due to

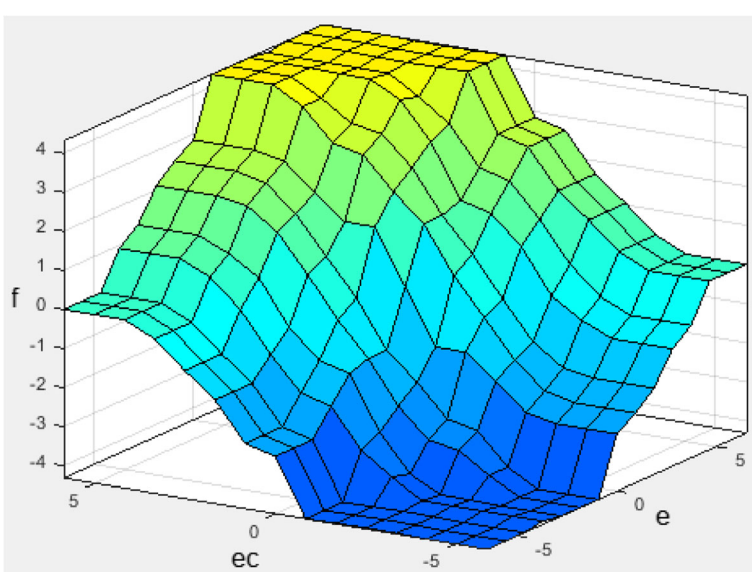

Fig. 4 Fuzzy logic rule—surface plot

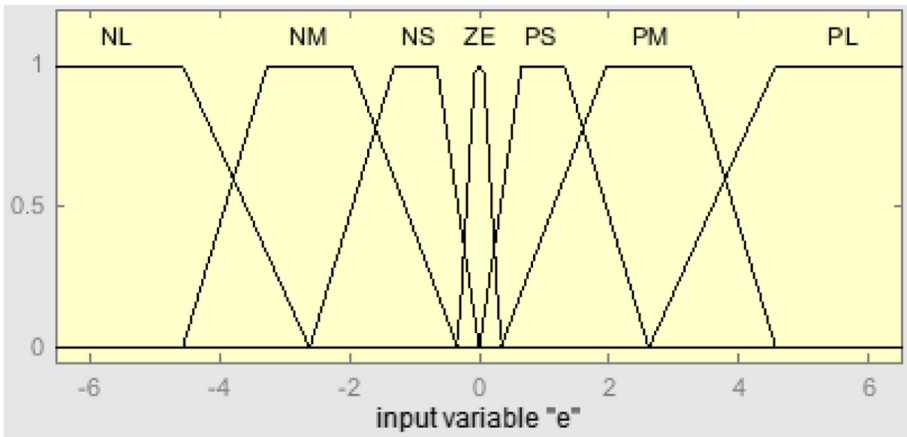

Fig. 5 Membership function (e)

random input, RMS suspension space travel is taken as one of the objective functions.

$$\text{Suspension Travel} = x_s - x_{us} \tag{6}$$

$$\text{RMS Suspension Travel} = \left\{\frac{1}{T}\int_0^T [(x_s(t) - x_{us}(t))]^2 dt\right\}^{\frac{1}{2}} \tag{7}$$

Dynamic tyre deflection

Dynamic tyre force is related to tyre deflection. Due to the random nature of input, the RMS of tyre deflection is the next objective function.

$$\text{Tyre Deflection} = x_{us} - x_r \tag{8}$$

$$\text{RMS Tyre Deflection} = \left\{\frac{1}{T}\int_0^T [(x_{us}(t) - x_r(t))]^2 dt\right\}^{\frac{1}{2}} \tag{9}$$

Control force is introduced as one of the objective functions, to find optimum control force to achieve ride comfort.

$$\text{RMS } f = \left\{\frac{1}{T}\int_0^T [(f(t))]^2 dt\right\}^{\frac{1}{2}} \tag{10}$$

According to Baumal et al. (1998), at least, 125 mm of suspension travel is required, and maximum seat acceleration should not increase 4.5 m/s^2 to avoid hitting the suspension stop. To minimize dynamic tyre forces, maximum tyre deflection should not increase 0.0508 m. These parameters are included as constraints in the optimization problem.

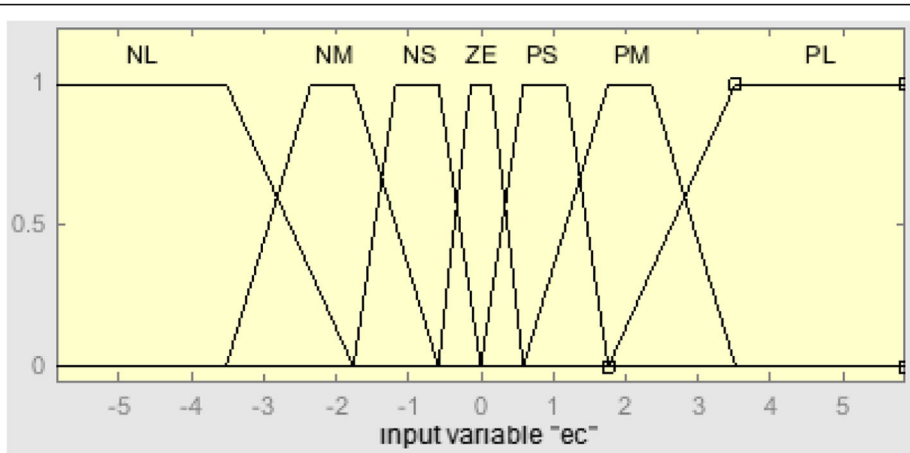

Fig. 6 Membership function (ec)

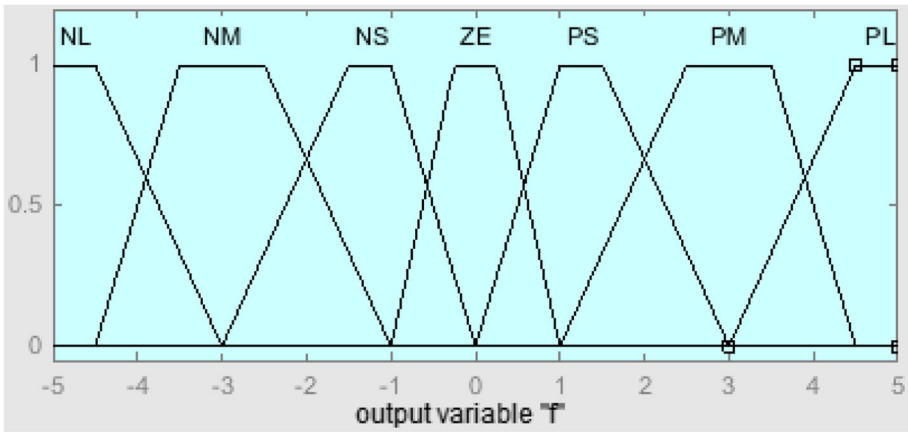

Fig. 7 Membership function (U)

The formulation of the optimization problem is as follows:

$$f_{\mathrm{obj1}} = \text{Minimize (RMS } f\text{)}$$

$$f_{\mathrm{obj2}} = \text{ Minimize (VDV}_{\mathrm{s}}\text{)}$$

$$f_{\mathrm{obj3}} = \text{ Minimize (A}_{\mathrm{ws}}\text{)}$$

$$f_{\mathrm{obj4}} = \text{ Minimize (RMS Suspension Travel)}$$

$$f_{\mathrm{obj5}} = \text{ Minimize (RMS Tyre Deflection)}$$

Subject to constraints:

$$a_{\mathrm{max_seat}} \le 4.5\frac{m}{\mathrm{s}^2},\ \mathrm{Max.}(x_{\mathrm{s}} - x_{\mathrm{us}}) \le 0.125\mathrm{m},$$

$$\mathrm{Max.}(x_{\mathrm{us}} - x_{\mathrm{r}}) \le 0.0508\mathrm{m}, f\max \le 2000\ \mathrm{N}.$$

Multi-objective optimization

Researchers have invented several meta-heuristic optimization algorithms to optimize the problems in several fields. These algorithms have implemented on several mathematical problems involving single objective optimization to multi-objective optimization and provided excellent results.

The suspension system has to perform several conflicting objectives such as ride comfort, road holding, and suspension/rattle space requirements. Thus, the optimization problem becomes a multi-objective type (consisting of RMS control force, VDV, RMS sprung mass acceleration, RMS suspension space requirement, and RMS dynamic tyre deflection as objective functions) with conflicts. As compared to a single objective optimization problem, a multi-objective optimization (MOO) problem has to satisfy several objectives simultaneously. Hence, multi-objective optimization using a genetic algorithm (GA) (Holland 1992; Holland 1975) is implemented to solve the optimization problem.

In the solution of MOO problems, MOO forms a Pareto optimal front consisting of multiple optimal solutions. GA is implemented to optimize in multiple domains as it handles complex optimization problems with discontinuities, non-differentials, noisy functions, and functions with multi-modality. GA also supports parallel computations with obtaining Pareto front in a single run. Non-dominated sort GA-II (NSGA-II) (Deb et al. 2002) is one of the MOEAs using GA strategy. NSGA-II implements non-dominated sort algorithm thus reducing the computational complexities. While sorting the parents and children, elitism is introduced in NSGA-II. In NSGA-II, to preserve the diversity and uniform spread of optimal front, a crowding distance (CD) (Deb et al. 2002) operator is used. Chromosomes with better fitness are assigned highest ranks, and thus, they determine the domination.

From the non-dominated front, parents are selected by tournament selection and compared to the CD. New

Table 2 Membership functions

MF	Input 1 (e)	Input 2 (ec)	Output (f)
NL	[− 1− 1 − 0.7 − 0.4]	[− 1 − 1 − 0.6 − 0.3]	[− 1 − 1 − 0.9 − 0.6]
NM	[− 0.7− 0.5 − 0.3 − 0.05]	[− 0.6 − 0.4 − 0.3 − 0.1]	[− 0.9 − 0.7 − 0.5 − 0.2]
NS	[− 0.4 − 0.2 − 0.1 0]	[− 0.3 − 0.2 − 0.1 0]	[− 0.6 − 0.3 − 0.2 0]
ZE	[− 0.05 − 0.01 0.01 0.05]	[− 0.1 − 0.025 0.025 0.1]	[− 0.2 − 0.05 0.05 0.2]
PS	[0 0.1 0.2 0.4]	[0 0.1 0.2 0.3]	[0 0.2 0.3 0.6]
PM	[0.05 0.3 0.5 0.7]	[0.1 0.3 0.4 0.6]	[0.2 0.5 0.7 0.9]
PL	[0.4 0.7 1 1]	[0.3 0.6 1 1]	[0.6 0.9 1 1]

Table 3 Design variables range—PID Control

Design variable	Range	Size	
Kp	15,000–2000 = 13,000	$2^{13} = 8192 < 13{,}000 < 2^{14} = 16{,}384$	14 bits
Ki	150–10 = 140	$2^{7} = 128 < 140 < 2^{8} = 256$	08 bits
Kd	50,000–15,000 = 35,000	$2^{15} = 32{,}768 < 35{,}000 < 2^{16} = 65{,}536$	16 bits

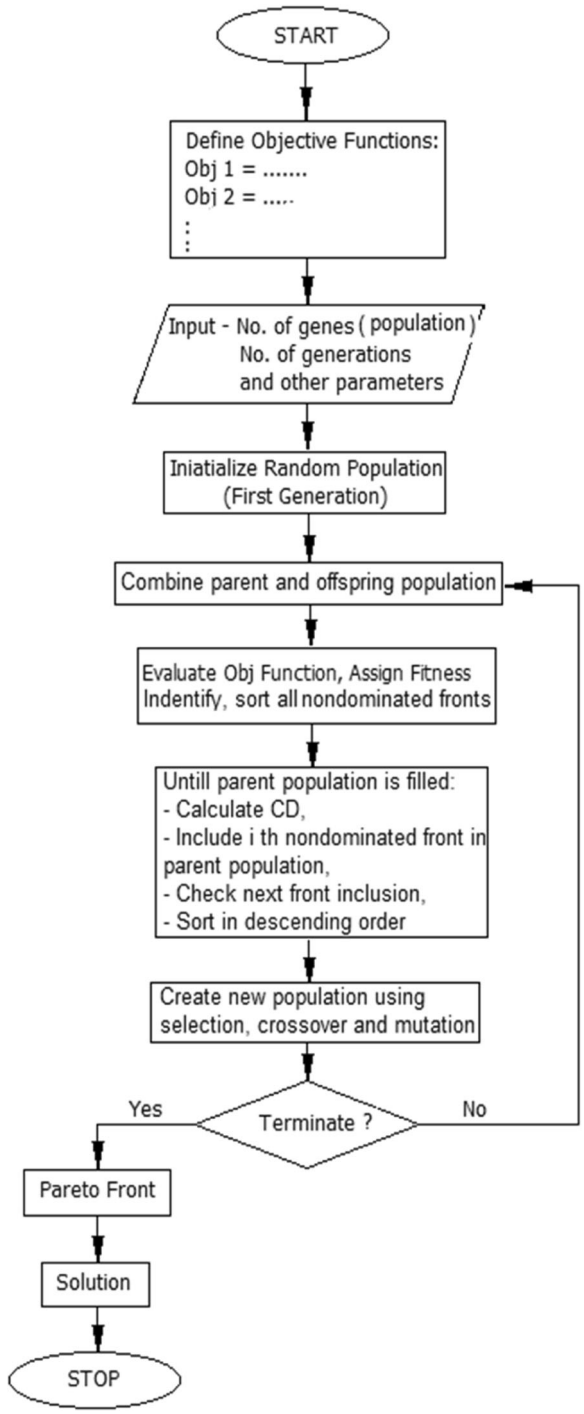

Fig. 8 Flow chart—GA (Nagarkar et al. 2016)

off-springs are created using a crossover operator and mutation operator. New off-springs and current population (parents) are combined to generate a new population. Selection is carried out for next generation individuals. The binary tournament selection method is used by NSGA-II to handle constraints. For multi-objective optimization, NGPM code (NSGA-II Program in Matlab) is used (Song 2011; Song 2015). NGPM is the implementation of NSGA-II (non-dominated sort genetic algorithm) in Matlab.

Table 4 ISO Road classification (ISO 8608 (1995))

Road class	Degree of roughness $\varphi(n_o)$ (10^{-6} m^2/(cycle/m)) Where $n_o = 0.1$ cycle/m		
	Lower limit	Geometric mean	Upper limit
A (very good)	–	16	32
B (good)	32	64	128
C (average)	128	256	512
D (poor)	512	1024	2048
E (very poor)	2048	4096	8196

Optimization methodology—PID control

During simulation and optimization of PID controller, PID parameters are randomly initialized, and objective functions are determined. Then, optimum PID parameters are iteratively obtained till algorithm stops. The classical PID gains are determined using the Z-N method.

Search space for PID controller is as follows -

$$Kp \in [2000, 15000], Ki \in [10, 150], Kd \in [15000, 50000.]$$

Optimization methodology—fuzzy logic control

FLC is a typical two input-one output functions controller. In this design, initially, seven trapezoidal membership functions are defined for two inputs and output. The seven membership functions are initialized in the range of [− 1 1] and are then multiplied using respective scale factors. Table 2 represents the initial membership functions in the range of [− 1 1]. Also, error (e), change in error (ec) and control output (f) are scaled using scaling factors ke, kec, and kf respectively and included in the Simulink® model.

During optimization, values are randomly initialized and the model is simulated to determine objective functions. Then, iteratively optimum parameters are obtained from their ranges till the algorithm stops.

The search space for the input-output functions and scaling factors is as follows:

$$\text{Input Function1} \in [1, 10], \text{Input Function2} \in [1, 10], \text{Output Function1} \in [1, 10]$$

$$ke \in [-5, 5], kec \in [-5, 5], kf \in [0, 25]$$

NSGA-II—population range

In GA, the range of design variable Kp is (15000−2000=) 13,000. Thus, the design variable Kp needs to be divided into 13,000 equal range of size. Hence, $2^{13} = 8192 <$

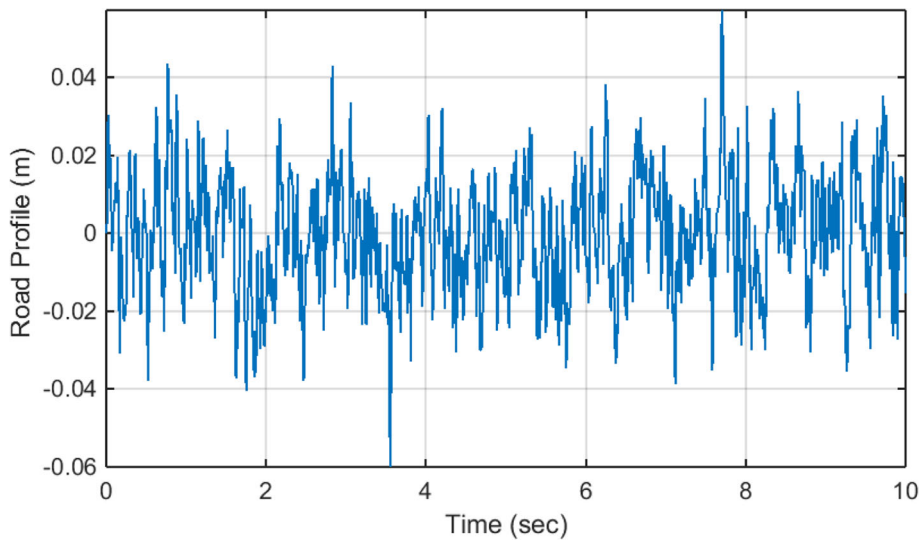

Fig. 9 Road surface (class C, velocity 80 kmph)

$13{,}000 < 2^{14} = 16{,}384$, i.e., 14 bits are required to store the value of design variable Kp in the chromosome. Similarly, for other design variables, the bit required is tabulated in Table 3.

Hence, the total length of chromosome or gene is $14 + 08 + 16 = 38$ bits that are required, where the first 14 bits are required for Kp, the next 08 bits are required for Ki, and the next 16 bits are required for Kd. Population size is selected such that

$N_s <$ population size $< 2N_s$, where $N_s =$ string length (Alander 1992)

Also, the range of variables for the FLC design variables is small as compare to the PID controller. Thus, selecting population size of 100 (Rosenthal and Borschbach 2014; Hernández-Díaz et al. 2008; Nagarkar et al. 2016) and optimization is stopped after 100 generations. Figure 8 explains the flowchart of the GA algorithm implemented for multi-objective optimization.

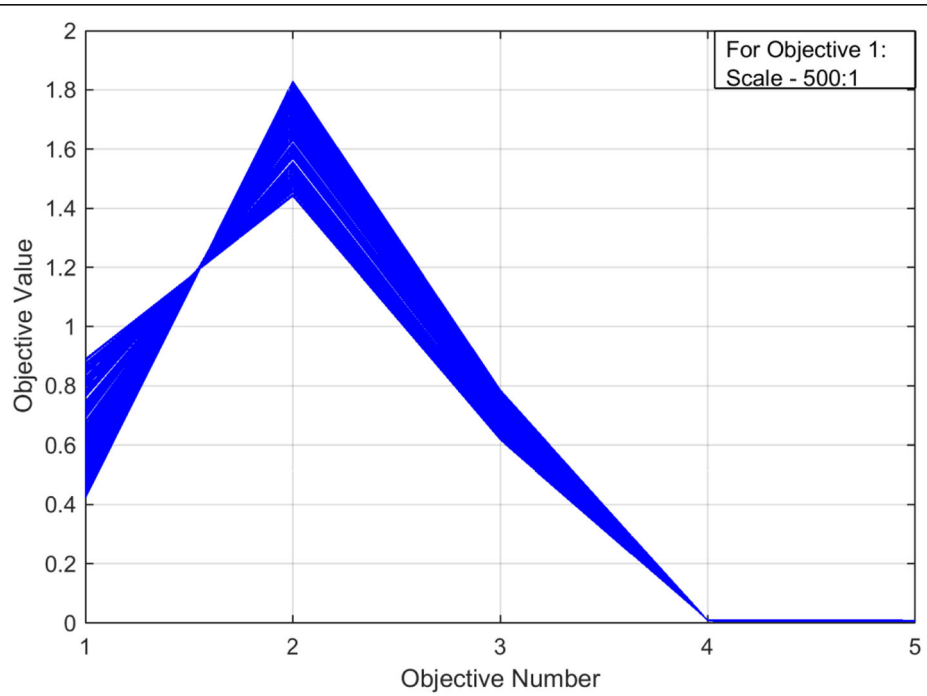

Fig. 10 Trade-off front—PID Control

Results and discussion

Multi-objective optimization of the non-linear quarter-car model is simulated in a Matlab/Simulink® environment using NSGA-II algorithm.

The stationary road roughness is effectively described by power spectral density (PSD). When a car moves at a constant velocity v, the road roughness can be viewed as a stationary process in the space domain. The differential equation of road roughness can be expressed as (He et al. 2008; Zhang et al. 2007):

$$\dot{x_r}(t) + 2\pi n_o v x_r(t) = \sqrt{S_q(n_o)v}\, w(t) \tag{11}$$

Equation (11) is modeled in the Simulink environment to model the road surface. According to ISO 8608, roads are divided into classes like A, B, C, D, and E. Class A and B represents expressways or motorways, whereas class C road is a typical average road type. Class B and C roads are generally country or district roads. Class C road considers velocities of typical secondary roads ranging from ~ 30 kmph to ~ 60 kmph. The input road condition is modeled as class C road (average road) with a degree of road roughness 512×10^{-6} $m^2/(cycle/m)$ (Zhang et al. 2007; ISO 8608 1995). Refer to Table 4 for the road roughness classification. The vehicle is traveling with a velocity of 80 kmph. Figure 9 represents the class C road surface.

PID controller

The trade-off front of 100 different solutions for objective functions satisfying the constraints is obtained after optimization. The trade-off front is shown in Fig. 10. For ride comfort and health criterion, RMS acceleration and VDV are selected as optimum values. Hence, for PID controller P, D and D parameters' gain values are selected for minimum valued of RMS acceleration and VDV and simulated further. Refer to Table 7 for the corresponding optimized PID parameters.

It is observed that the RMS acceleration for the GA-optimized PID controller is 0.6178 m/s^2, which is a little uncomfortable. In GA-PID controlled system, RMS acceleration is reduced by 34% (passive suspension system has RMS acceleration 0.9322 m/s^2 which is uncomfortable) and is reduced by 10% as compared to the classical PID control. For GA optimized PID controller, VDV is reduced by 33% as compared to the passive suspension system and is reduced by 11% as compared to classical PID control. Also, constraints are not violated in the GA optimized system. The results of RMS optimal control force, RMS sprung mass acceleration, RMS suspension space, RMS tyre deflection, maximum controller force, and maximum sprung mass acceleration are tabulated in Table 5 (refer to Fig. 11 for time domain results).

Further frequency domain analysis is carried out for the PID controlled system and passive system. In frequency analysis, it is observed that the optimized PID controlled system experiences low amplitudes of body accelerations as compared to the passive suspension system (refer to Fig. 12). PID can reduce the amplitude of body accelerations at points 10^0 and 10^1 Hz frequencies. Also, it shows better performance over higher amplitude regions > 10 Hz.

Fuzzy logic control

During simulation 2-DOF nonlinear active suspension system, it is excited by a random road disturbance. The NSGA-II-based optimization is carried out and results are obtained using a MATLAB/SIMULINK. The velocity and acceleration of sprung mass are selected as an error (e) and change in error (ec) feedback signals for the 2-DOF suspension system control.

The trade-off front of 100 different solutions for objective functions satisfying the constraints is obtained after optimization. The trade-off front is shown in Fig. 13. For ride comfort and health criterion, the minimum RMS acceleration and VDV are selected as optimum values. Hence, FLC parameters, ke, kc, kf, and scaling factors for input-output membership functions are selected having minimum values of RMS acceleration and VDV corresponding to the trade-off front and

Table 5 Optimization results—objective function and constraints

Parameter	Fuzzy logic control-GA	PID-GA	PID classical	Passive system
RMS control force (*N*)	140.9662	445.4385	346.8979	–
VDV ($m/s^{1.75}$)	1.1782	1.4410	1.6174	2.1509
Aw (m/s^2)	0.5057	0.6178	0.6890	0.9322
RMS suspension space deflection (m)	0.0085	0.01007	0.008700	0.009311
RMS tyre deflection (m)	0.0042	0.008864	0.007300	0.004473
Max control force (N)	345.6605	1423.1810	1173.24400	–
Max acceleration (m/s^2)	2.31900	1.8615	2.1800	3.16720
Max suspension space deflection (m)	0.02520	0.03426	0.03050	0.02640
Max tyre deflection (m)	0.01350	0.02639	0.02510	0.01840

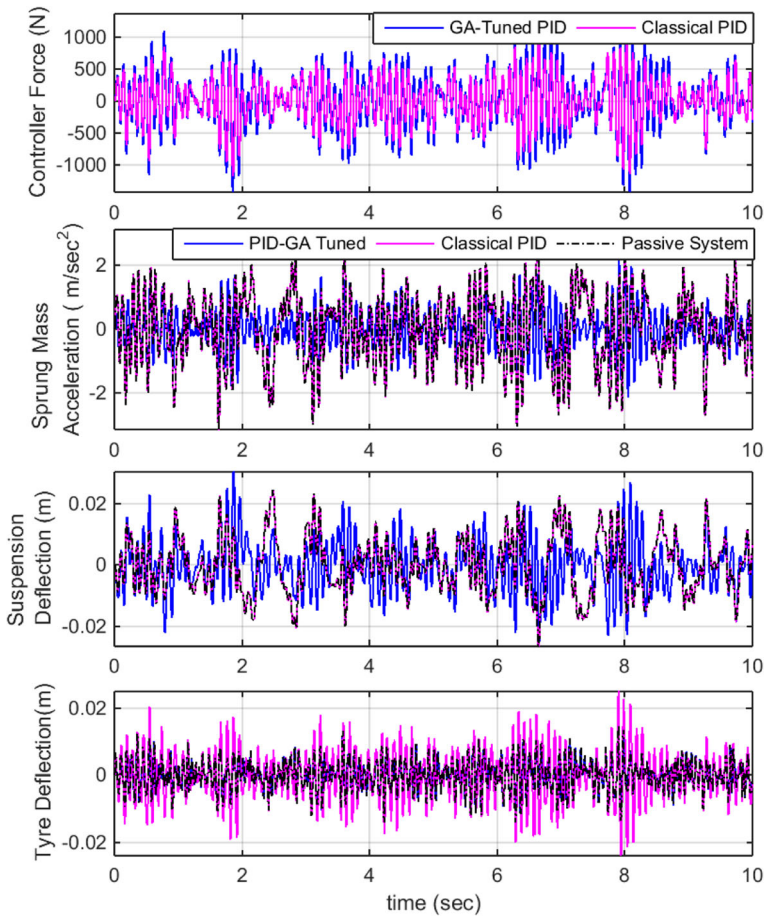

Fig. 11 PID control results—time domain

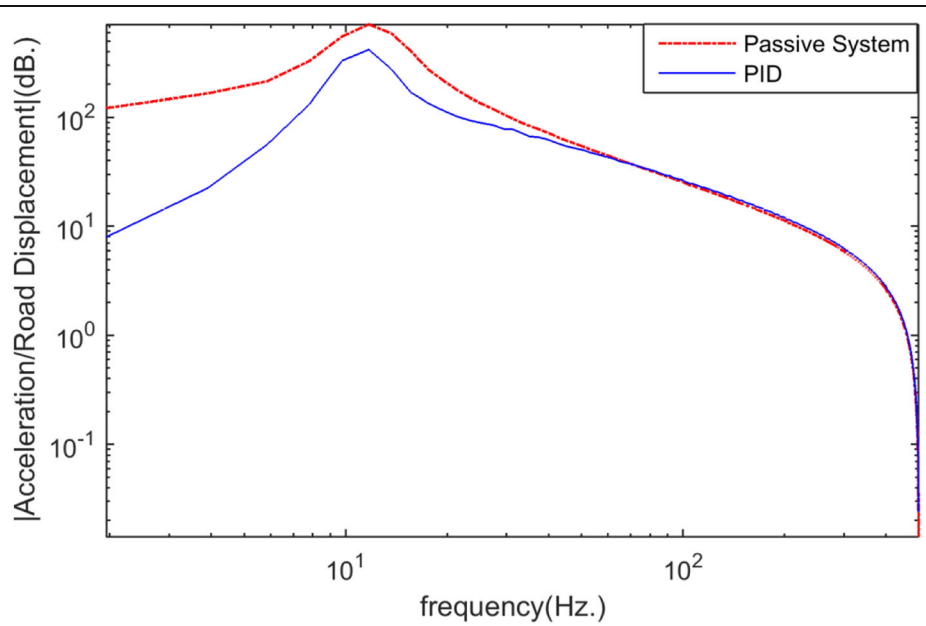

Fig. 12 PID control results—frequency domain

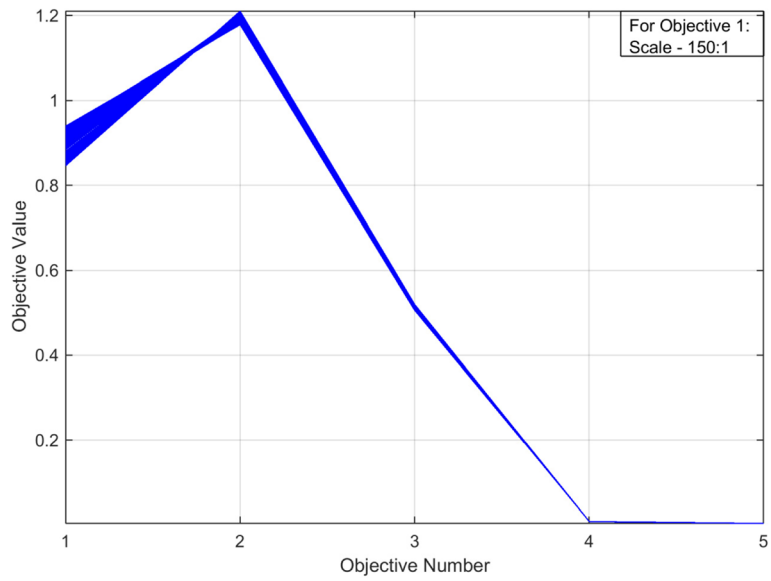

Fig. 13 Trade-off front—fuzzy logic control

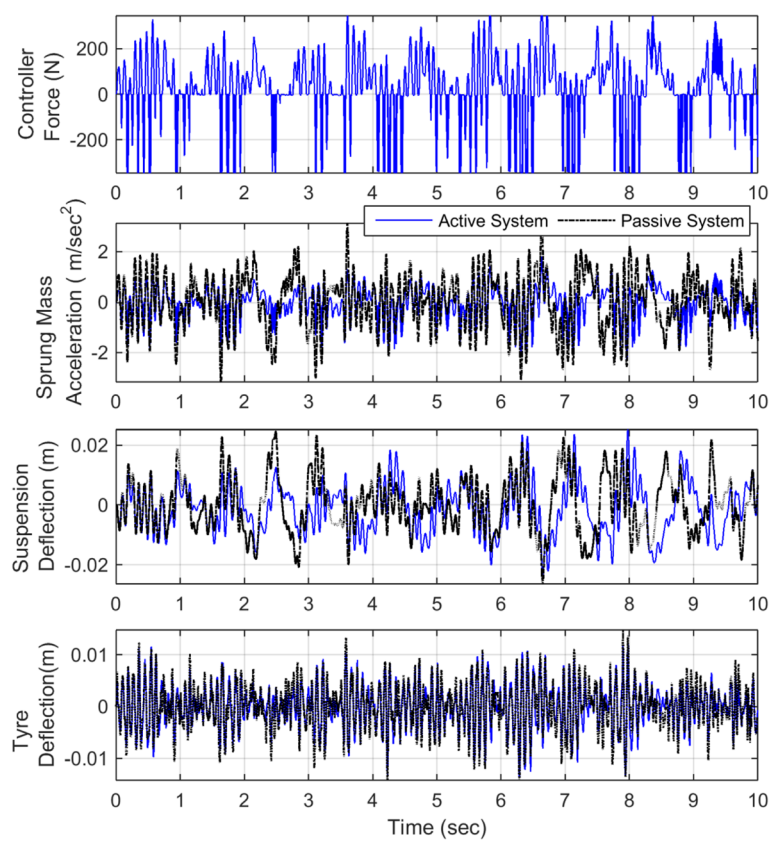

Fig. 14 Fuzzy logic control results—time domain

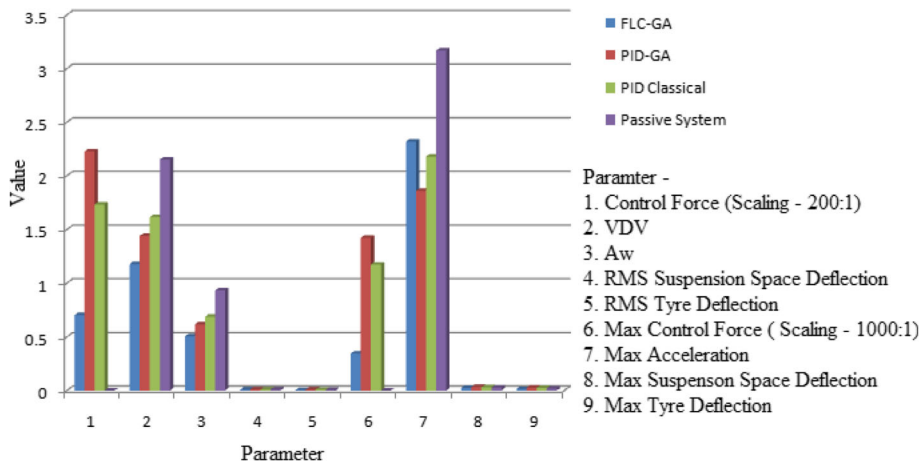

Fig. 15 Optimization results—objective functions and constraints

are simulated further. Refer to Table 7 for the corresponding optimized FLC parameters.

It is observed that RMS acceleration for the GA-optimized FLC is 0.5057 m/s^2, which is a little uncomfortable. In the fuzzy logic control system, RMS acceleration is reduced by 46% as compared to the passive system (passive suspension system has RMS acceleration 0.9322 m/s^2 which is uncomfortable) and by 18% as compared to GA-based PID controller. Also, VDV for GA-based FLC is reduced by 45% as compared to the passive suspension system and by 18% as compared to the GA-based PID controller. Also, the RMS suspension space and RMS tyre deflection are less for FLC as compared to the GA-based PID controller and passive suspension system. The constraints are not violated in GA optimized FLC. The results of RMS optimal control force, RMS sprung mass acceleration, RMS suspension space, RMS dynamic tyre deflection, and maximum controller force are maximum sprung mass acceleration are tabulated in Table 5 (refer to Fig. 14 for the time domain results). Results are also shown in the bar chart (refer to Fig. 15).

From simulations and Table 5, it is observed that the GA-tuned FLC controller performs better as compared to the GA-tuned PID controller. In the case of GA-tuned FLC controller, VDV and RMS acceleration is

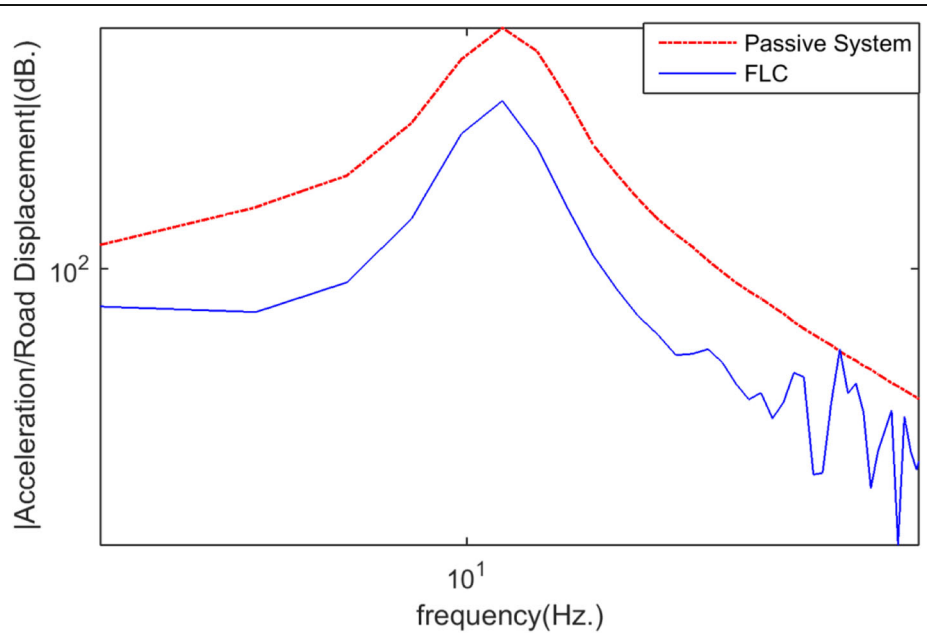

Fig. 16 Fuzzy logic control results—frequency domain

reduced by 18.23% and 18.14% as compared to the GA-tuned PID controller. Also, RMS suspension space deflection and RMS tyre deflection is less for the GA-tuned FLC controller.

Further, the frequency domain analysis is also carried out for the FLC system and passive system. For frequency analysis, it is observed that the FLC system experiences low amplitudes of vibrations over a broader range of frequencies as compared to the passive suspension system (refer to Fig. 16). The FLC can reduce the amplitude of body accelerations at points 10^0 and 10^1 Hz frequencies and also shows better performance over higher amplitude regions > 10 Hz.

Further, to study the controller performance, the nonlinear quarter car suspension system is simulated over class C and class D roads with vehicle speed ranging from 20 to 160 kmph. Figure 17 shows performance over class C road type. For class C road, the maximum value of VDV is 1.8385 $m/s^{1.75}$ and is observed at 160 kmph, for GA-tuned PID controller. Whereas for the GA-based FLC maximum VDV is 1.7205 $m/s^{1.75}$. The maximum value of RMS sprung mass acceleration is 0.7910 m/s^2 for the GA-tuned PID controller and 0.7065 m/s^2 for the GA-FLC controller and is observed at 160 kmph. From Fig. 17, it is observed that, for FLC controller, up to 130 kmph speed, the RMS sprung mass acceleration is in a slightly uncomfortable region as per ISO2631-1:1997. Whereas for the PID controller, the same level is achieved up to 100 kmph. Above these speed limits, the RMS sprung mass acceleration falls under the fairly uncomfortable region. Other parameters like RMS suspension space and RMS tyre deflection are also represented in Fig. 17.

The non-linear quarter car is also simulated over class D road. Figure 18 shows the performance of the nonlinear quarter car with both controllers over class D road. From the figure, it is observed that FLC and PID controller shows nearly the same performance for the RMS sprung mass acceleration. The VDV value is maximum at 160 kmph for both controllers. The maximum VDV

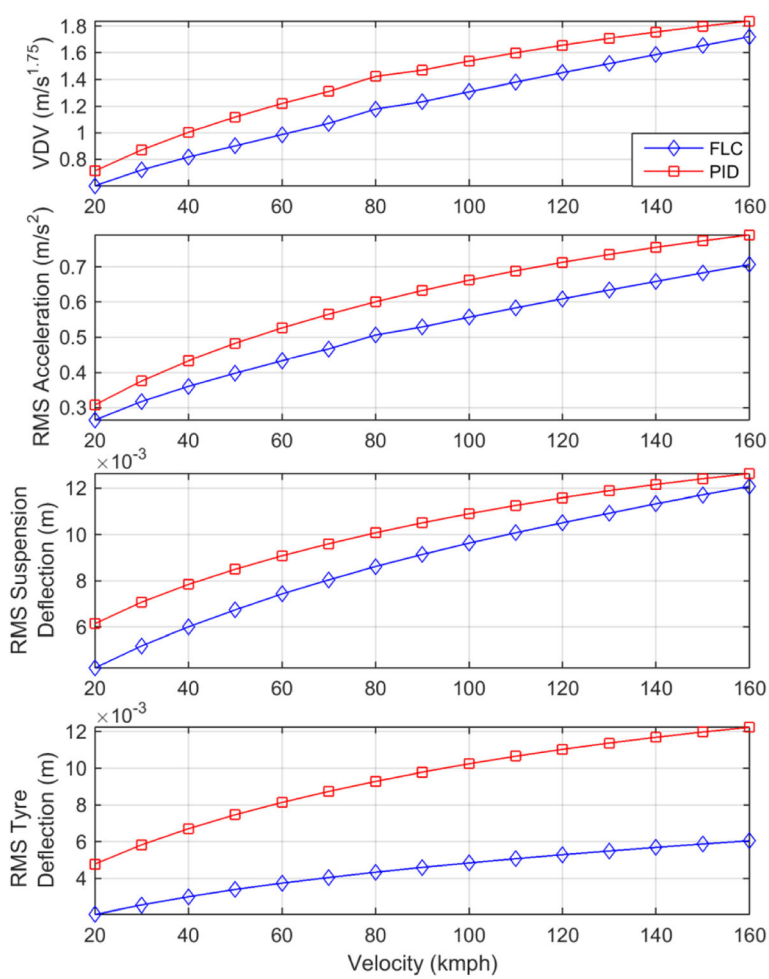

Fig. 17 Performance of FLC and PID controller—class C road

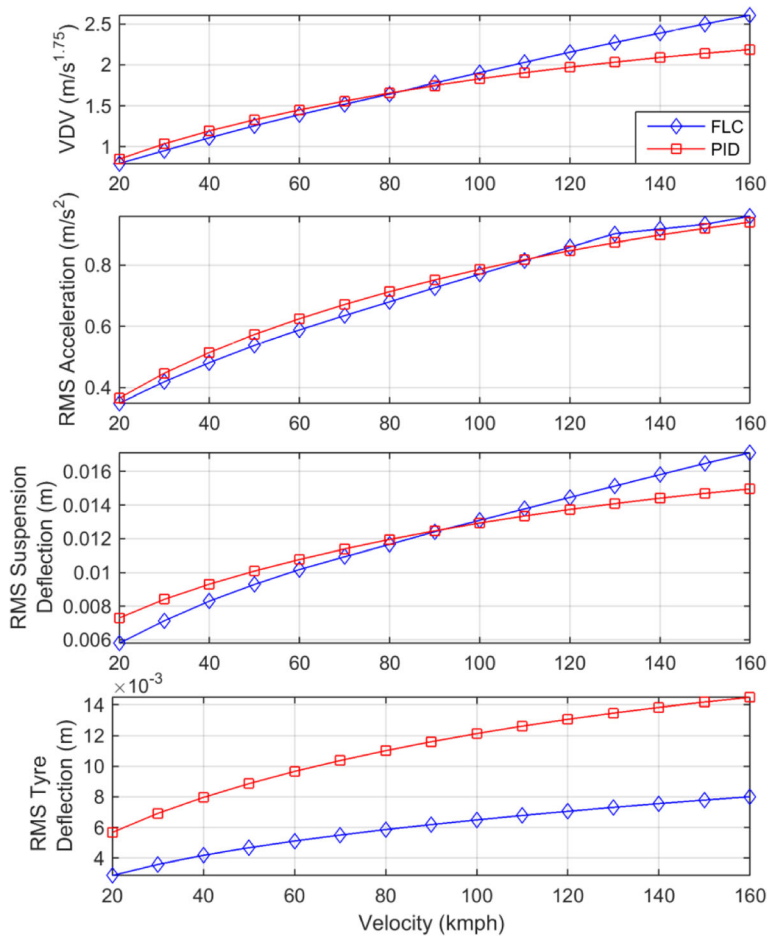

Fig. 18 Performance of FLC and PID controller—class D road

for PID controller is 2.1874 m/s$^{1.75}$ and for FLC controller VDV is on the slightly higher side and is 2.6091 m/s$^{1.7}$. The maximum RMS sprung mass is the acceleration is observed at 160 kmph for both controllers and is 0.9391 m/s^2 for the GA-tuned PID controller and 0.9586 m/s^2 for GA-FLC controller respectively. From Fig. 18, it is observed that for FLC controller, up to 80 kmph speed, the RMS sprung mass acceleration is in a slightly uncomfortable region whereas for PID controller, the same level is achieved up to 70 kmph as per ISO2631-1:1997. Above these speed limits, RMS sprung mass acceleration falls under the fairly uncomfortable region.

Table 6 Human model results—FLC, PID, and passive system

Parameter	FLC	PID	Passive system
VDV_h (m/s$^{1.75}$)	2.8938	2.8787	4.8180
Aw_h (m/s^2)	1.1083	1.1082	2.0408
CF	2.6811	3.3829	3.3109
AR_h	0.9684	1.0192	1.2033
AR_ut	0.9345	1.0277	1.1969

To check the effect of vibrations on a human body, the suspension system along with the human model is simulated. The nonlinear quarter car along with seat and human model is simulated using PID and FLC system and compared with a passive system. VDV at the head, RMS head acceleration, crest factor, and amplitude ratios are observed.

Crest factor (CF) is defined as the ratio of maximum head acceleration to the RMS head acceleration [26].

$$\mathrm{CF} = \mathrm{Max}\left(a_{\mathrm{h}}\right) / \left\{\frac{1}{\mathrm{T}} \int_0^{\mathrm{T}} \left[a_{\mathrm{wh}}(t)\right]^2 \mathrm{dt}\right\}^{\frac{1}{2}} \tag{12}$$

The amplitude ratio of head RMS acceleration to seat RMS acceleration (AR_h) is defined as the ratio of the RMS head acceleration to the RMS seat acceleration (Nagarkar et al. 2016).

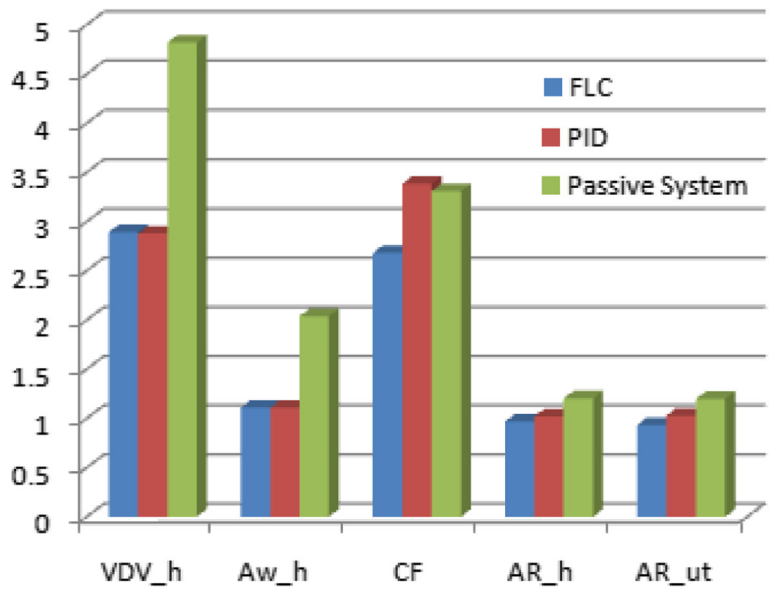

Fig. 19 Human model results

$$\mathrm{AR_h} = \left\{\frac{1}{\mathrm{T}}\int_0^{\mathrm{T}}[a_{\mathrm{h}}(t)]^2\mathrm{dt}\right\}^{\frac{1}{2}} / \left\{\frac{1}{\mathrm{T}}\int_0^{\mathrm{T}}[a_{\mathrm{s}}(t)]^2\mathrm{dt}\right\}^{\frac{1}{2}} \tag{13}$$

The amplitude ratio of upper torso RMS acceleration to seat RMS acceleration (AR_ut) is defined as the ratio of the RMS upper torso acceleration to the RMS seat acceleration (Nagarkar et al. 2016).

$$\mathrm{AR} = \left\{\frac{1}{\mathrm{T}}\int_0^{\mathrm{T}}[a_{\mathrm{ut}}(t)]^2\mathrm{dt}\right\}^{\frac{1}{2}} / \left\{\frac{1}{\mathrm{T}}\int_0^{\mathrm{T}}[\mathrm{a_s}(t)]^2\mathrm{dt}\right\}^{\frac{1}{2}} \tag{14}$$

It is observed that the RMS head acceleration is reduced by 39% in the case of the GA-based FLC and reduced by 46% in the case of the GA-based PID controller as compared to the passive suspension system, whereas VDV at the head is reduced by 39% and 41% for

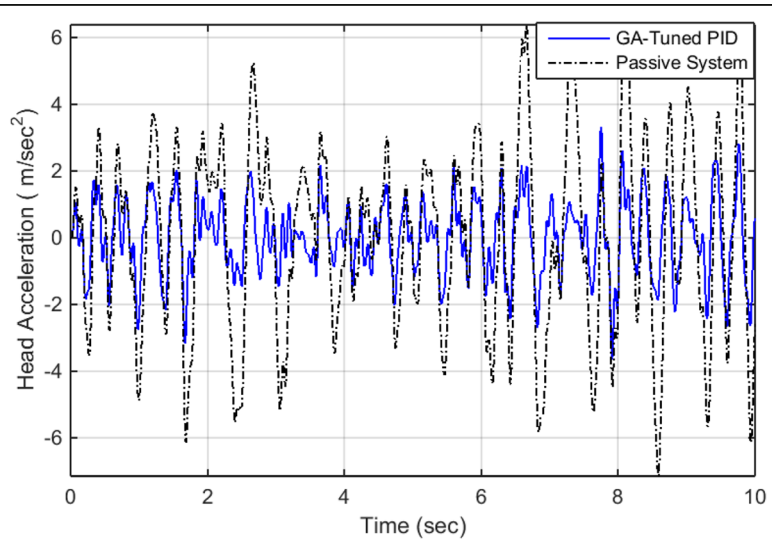

Fig. 20 Head acceleration time domain results—PID and passive suspension system

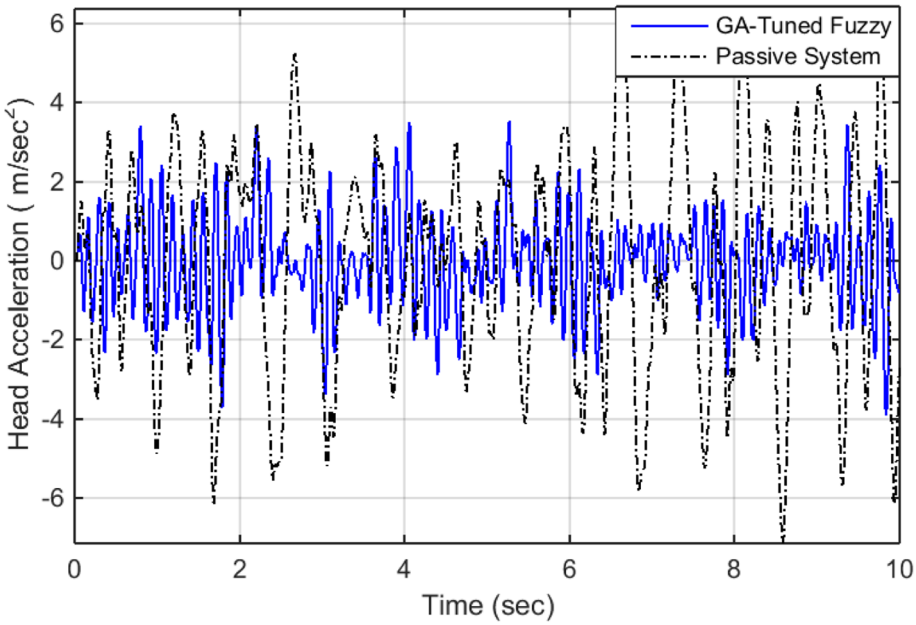

Fig. 21 Head acceleration time domain results—FLC and passive suspension system

FLC and PID controller as compared to the passive system. CF, AR_h, and AR_ut parameters are reduced for FLC as compared to the PID and passive suspension system. Results are tabulated in Table 6 and are presented in the bar chart (refer to Fig. 19).

From Table 6 and Fig. 19, it is observed that the GA-tuned FLC has RMS acceleration of head and VDV at head slightly greater (1.9% and 1% respectively) as compared to the GA-tuned PID controller. But, FLC gives better results as compared to the PID controller for CF, AR_h, and, AR_ut (20.75%, 4.98%, and 9.07% less respectively as compared to PID controller).

From frequency domain results, it is observed that the PID controller experiences low amplitude of vibrations at the head as compared to the passive system. FLC also

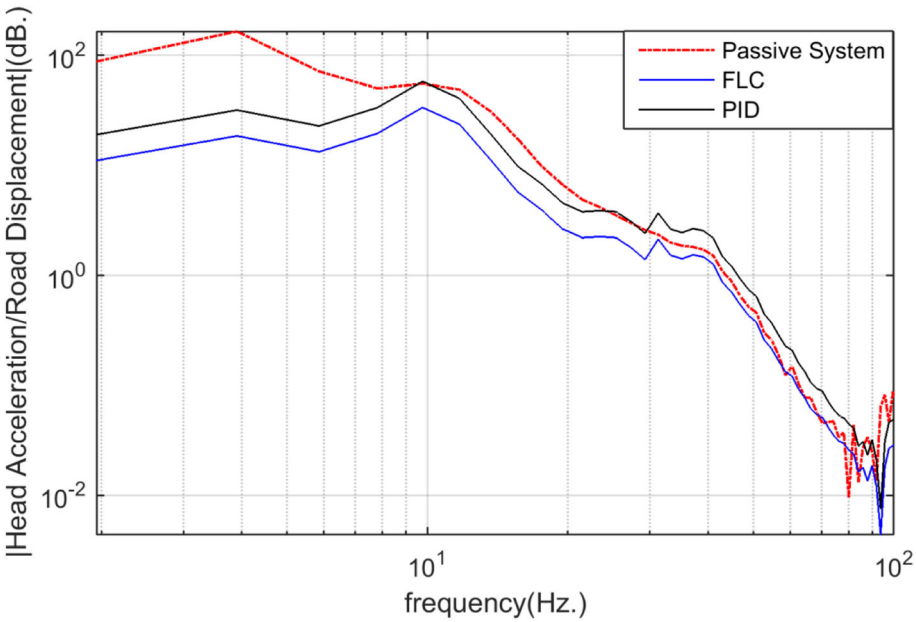

Fig. 22 Head acceleration frequency domain results—FLC, PID, and passive suspension system

Table 7 Controller parameters after optimization

Type	Controller parameters
PID	Classical: KP = 3055, KI = 0.7; KD = 32,060.
	Optimized: KP = 200, KI = 50.9245; KD = 48,176.4
FLC	Ke = −0.2806, Kec = −4.0721; Ku = 15.9754,
	Input Function1 = 6.5270, Input Function2 = 5.8651; Output Function = 5

experiences low amplitude of vibrations at a broader range of frequencies. FLC and PID controller improves amplitude of vibrations at head around 10^0 Hz regions, which is the most sensitive region related to ears and eyes. Refer Figs. 20 and 21 for time domain results and Fig. 22 for frequency domain results.

Conclusions

This paper presents mathematical modelling, control, and multi-objective optimization of an active nonlinear quarter car suspension system. A nonlinear 2-DoF nonlinear quarter car model having quadratic nonlinearities in the tyre and cubic nonlinearity in suspension spring is developed and implemented for control applications.

The PID and FLC strategies are implemented on a nonlinear quarter car system. Controller parameters such as P, I, and D parameters of the PID controller and input-output membership functions' range and scaling factors of the FLC are then tuned using NSGA-II algorithm (Table 7). In optimization problem comfort and health criterion consisting of VDV, RMS acceleration, along with stability criterions consisting of suspension space and tyre deflection are used as objective functions. ISO 2631-1 methodology is adopted and successfully implemented. Numerical simulations show that the GA-based FLC active control system minimizes the frequency-weighted RMS acceleration and VDV as compared to the PID and passive suspension system thus improving the ride comfort. Results are also presented in the frequency domain which shows that the active control system experiences less amplitude as compared to the passive one.

Further results are extended on a human model, which shows that the active control system shows minimum RMS head acceleration, VDV at the head, crest factor, and amplitude ratio at the head and amplitude ration at upper torso, thus providing comfort with health criterion.

Abbreviations

A_w: Frequency-weighted RMS head acceleration (m/s^2); a_w: Frequency-weighted sprung mass acceleration (m/s^2); c: Damping coefficient (Ns/m); c_h: Cervical spine damping (Ns/m); c_{lt}: Lumber spine damping (Ns/m); c_{ut}: Thoracic spine damping (Ns/m); *f*: Control force (N); f_{obj}: Objective function; k: Stiffness (N/m); ke, kec, ku: Scaling factors for error, change in error, and force respectively; k_h: Cervical spine stiffness (N/m); k_{lt}: Lumber spine stiffness (N/m); Kp, Ki, Kd: PID gains—proportional, integral, and derivative respectively; k_{snl}: Nonlinear spring stiffness (N/m^3); k_t: Tyre stiffness (N/m); k_{tnl}: Nonlinear tyre stiffness (N/m2); k_{ut}: Thoracic spine stiffness (N/m); m: Mass (kg); n_o: Reference spatial frequency = 0.1(cycles/*m*); $Sq(n_o)$: Coefficient of road roughness; v: Velocity (m/s); VDV: Vibration dose value (m/s$^{1.75}$); w(t): White noise signal having PSD = 1; x, $\dot{x}$, $\ddot{x}$: Displacement (m), velocity (m/s), and acceleration (m/s^2); x_r: Road profile (m);

Subscripts

c: Seat cushion; f: Frame; h: Head; lt: Lower torso; s: Sprung; t: Thigh and pelvis; us: Unsprung; ut: Upper torso

Acknowledgements

The first author likes to express his deep gratitude towards the management of Ahmednagar Jilha Maratha Vidya Prasarak Smamaj, Ahmednagar, and likes to thank the Principal, SCSMCoE, Ahmednagar, for their encouragement and constant support to carry out this research work. The first author also likes to thank Springer Nature and Springer Nature Waiver team for their generous help and constant support during this work.

Funding

Not applicable.

Availability of data and materials

Not applicable.

Authors' contributions

MPN has been involved in the optimization, simulation, and drafting. YJB, GJV, and RNZ have been involved in the drafting of the manuscript and revising it critically for important intellectual content. All authors read and approved the final manuscript.

Competing interests

The authors declare that they have no competing interests.

Publisher's Note

Springer Nature remains neutral with regard to jurisdictional claims in published maps and institutional affiliations.

Author details

[1]SCSM College of Engineering, Ahmednagar, MS 414005, India. [2]Research Department of Mechanical Engineering, AVCoE, Sangamner, MS, India. [3]Professor, Mechanical Engineering Department, MIT Academy of Engineering, Alandi, Pune, MS 412105, India. [4]DVVP CoE, Vilad Ghat, Ahmednagar, MS 414111, India.

Received: 21 July 2018 Accepted: 25 October 2018
Published online: 22 November 2018

References

Abdelrassoul, R., Ali, Y., & Zaghloul, M. S. (2016). Genetic algorithm-optimized PID controller for better performance of PV system. In *Proceedings - 2016 world symposium on computer applications and research, WSCAR 2016* (pp. 18–22). https://doi.org/10.1109/WSCAR.2016.14.

Alander, J. T. (1992). On optimal population size of genetic algorithms. In *CompEuro 1992 Proceedings computer systems and software engineering* (pp. 65–70). https://doi.org/10.1109/CMPEUR.1992.218485.

Amato, F. J. D., & Viassolo, D. E. (2000). Fuzzy control for active suspensions. *Mechatronics, 10*(8), 897–920. https://doi.org/10.1016/S0957-4158(99)00079-3.

Baumal, A. E., McPhee, J. J., & Calamai, P. H. (1998). Application of genetic algorithms to the design optimization of an active vehicle suspension system. *Computer Methods in Applied Mechanics and Engineering, 163*(1–4), 87–94. https://doi.org/10.1016/S0045-7825(98)00004-8.

Boileau, P., & Rakheja, S. (1998). Whole-body vertical biodynamic response characteristics of the seated body biodynamic response under vertical vibration. *Journal of Sound and Vibrations, 215*(4), 841–862. https://doi.org/10.1016/S0169-8141(97)00030-9.

Bouarroudj, N., Boukhetala, D., Djari, A., Rais, Y., & Benlahbib, B. (2017). FLC based Gaussian membership functions tuned by PSO and GA for MPPT of photovoltaic system: a comparative study. In *2017 6th international conference on systems and control, ICSC 2017* (pp. 317–322). https://doi.org/10.1109/ICoSC.2017.7958640.

Bovenzi, M. (2005). Health effects of mechanical vibrations. *Giornale Italiano di Medicina del Lavoro ed Ergonomia, 27*(1), 58–64.

Celin, P. S., & Rajeswari, K. (2012). GA tuned Type-2 fuzzy logic controller for vehicle suspension system. In *Proceedings: international conference on computing, electronics and electrical technologies [ICCEET]* (pp. 383–388). Kumaracoil. https://doi.org/10.1109/ICCEET.2012.6203863.

Chen, H., & Chang, S. (2006). Genetic algorithms based optimization design of a PID controller for an active magnetic bearing. *IJCSNS International Journal of Computer Science and Network Security, 6*(12), 95–99.

Deb, K., Pratap, A., Agarwal, S., & Meyarivan, T. (2002). A fast and elitist multiobjective genetic algorithm: NSGA-II. *IEEE Transactions on Evolutionary Computation, 6*(2), 182–197. https://doi.org/10.1109/4235.996017.

Fuller, C. R., Elliott, S. J., & Nelson, P. A. (1996). *Active control of vibrations*. London: Academic Press.

Gad, S., Metered, H., Bassuiny, A., & Abdel Ghany, A. (2017). Multi-objective genetic algorithm fractional-order PID controller for semi-active magnetorheologically damped seat suspension. *Journal of Vibration and Control, 23*(8), 1248–1266. https://doi.org/10.1177/1077546315591620.

He, L., Qin, G., Zhang, Y., & Chen, L. (2008). Non-stationary random vibration analysis of vehicle with fractional damping. *2008 International Conference on Intelligent Computation Technology and Automation (ICICTA), 2*, 150–157. https://doi.org/10.1109/ICICTA.2008.348.

Hernández-Díaz, A. G., Coello, C. A. C., Pérez, F., Caballero, R., Molina, J., & Santana-Quintero, L. V. (2008). Seeding the initial population of a multi-objective evolutionary algorithm using gradient-based information. In *2008 IEEE congress on evolutionary computation, CEC 2008* (pp. 1617–1624). https://doi.org/10.1109/CEC.2008.4631008.

Holland, J. H. (1975). *Adaptation in natural and artificial systems*. Michigan: MIT Press.

Holland, J. H. (1992). Genetic algorithms. *Scientific American, 267*(1), 66–72. https://doi.org/10.1038/scientificamerican0792-66.

Huang, S. J., & Chao, C. H. (2000). Fuzzy logic controller for a vehicle active suspension system. *Proceedings of the Institution of Mechanical Engineers, Part D: Journal of Automobile Engineering, 214*(1), 1–12. https://doi.org/10.1243/0954407001527178.

ISO 2631-1 (1997) Mechanical vibration and shock - Evaluation of human exposure to whole-body vibration.

ISO 8608. (1995). *Mechanical vibration – Road surface profile – Reporting of measured data* (1st ed.).

Kalaivani, R., Lakshmi, P., & Sudhagar, K. (2014). Hybrid (DEBBO) fuzzy logic controller for quarter car model. In *Proceedings - UKACC international conference on control* (pp. 301–306). Loughborough.

Kesarkar, A. A., & Selvaganesan, N. (2015). Tuning of optimal fractional-order PID controller using an artificial bee colony algorithm. *Systems Science and Control Engineering, 3*(1), 99-105. https://doi.org/10.1080/21642583.2014.987480.

Li, P., & Du, X. (2006). A GA optimization for FLC with its rule base and scaling factors adjustment. In *Proceedings: International Conference on Intelligent Computing-Part II* (pp. 1–10). Kunming. https://doi.org/10.1007/11816171_1.

Liu, Y.-H., Wang, S.-C., & Peng, B.-R. (2016). Determining optimal membership functions of a FLC-based MPPT algorithm using the particle swarm optimization method. In *Proceedings - 2016 5th IIAI international congress on advanced applied informatics, IIAI-AAI 2016*. https://doi.org/10.1109/IIAI-AAI.2016.123.

Lixia, J., & Wanxiang, L. (2008). Chaotic vibration of a nonlinear quarter -vehicle model. In *Proceedings - IEEE vehicle power and propulsion conference* (pp. 1–4). Harbin.

McGee, C., Haroon, M., Adams, D., & Luk, Y. (2005). A frequency domain technique for characterizing nonlinearities in a tire-vehicle suspension system. *Journal of Vibration and Acoustics, 127*(1), 61–76. https://doi.org/10.1115/1.1855931.

Metered, H., Elsawaf, A., Vampola, T., & Sika, Z. (2015). Vibration control of MR-damped vehicle suspension system using PID controller tuned by particle swarm optimization. *SAE International Journal of Passenger Cars - Mechanical Systems, 8*(2), 01–0622. https://doi.org/10.4271/2015-01-0622.

Nagarkar, M. P., Vikhe Patil, G. J., & Zaware Patil, R. N. (2016). Optimization of nonlinear quarter car suspension–seat–driver model. *Journal of Advanced Research, 7*(6), 991–1007. https://doi.org/10.1016/j.jare.2016.04.003.

Niu, X. (2014). The optimization for PID controller parameters based on genetic algorithm. *Applied Mechanics and Materials, 513-517*, 4102–4105. https://doi.org/10.4028/www.scientific.net/AMM.513-517.4102.

Rajendiran, S., & Lakshmi, P. (2016). Simulation of PID and fuzzy logic controller for integrated seat suspension of a quarter car with driver model for different road profiles. *Journal of Mechanical Science and Technology, 30*(10), 4565–4570. https://doi.org/10.1007/s12206-016-0927-6.

Rosenthal, S., & Borschbach, M. (2014). Impact of population size and selection within a customized NSGA-II for biochemical optimization assessed on the basis of the average cuboid volume indicator. In *Proceedings - Sixth International conference on bioinformatics, biocomputational systems and biotechnologies* (pp. 1–7). Chamonix: BIOTECHNO.

Salem, M. M. M., & Aly, A. A. (2009). Fuzzy control of a quarter-car suspension system. *World Academy of Science, Engineering and Technology, 53*, 258–263.

Song, L. (2011). *NGPM-A NSGA-II Program in Matlab - User Manual. Version 4.1* (pp. 1–20).

Song, L. (2015). NGPM-A NSGA-II Program in Matlab v14. Matlab Code. http://in.mathworks.com/matlabcentral/fileexchange/31166-ngpm-a-nsga-ii-program-in-matlab-v1-4. Accessed on 15 Mar 2015.

Talib, M. H. A., & Darus, I. Z. M. (2014). Development of fuzzy logic controller by particle swarm optimization algorithm for semi-active suspension system using magneto-rheological damper. *WSEAS Transactions on Systems and Control, 9*, 77–85.

Tammam, M. A., Magdy, A. S., Aboelela, M. A., Moustafa, & Seif, A. E. A. (2013). A multi-objective genetic algorithm based PID controller for load frequency control of power systems. *International Journal of Emerging Technology and Advanced Engineering, 3*(12), 463–467.

Taskin, Y., Hacioglu, Y., & Yagiz, N. (2007). The use of fuzzy-logic control to improve the ride comfort of vehicles. *Strojniski Vestnik/Journal of Mechanical Engineering, 53*(4), 233–240.

Taskin, Y., Hacioglu, Y., & Yagiz, N. (2017). Experimental evaluation of a fuzzy logic controller on a quarter car test rig. *Journal of Brazilian Society of Mechanical Science and Engineering, 39*(7), 2433–2445. https://doi.org/10.1007/s40430-016-0637-0.

Van Niekerk, J. L., Pielemeier, W. J., & Greenberg, J. A. (2003). The use of SEAT effective amplitude transmissibility (SEAT) values to predict dynamic seat comfort. *Journal of Sound and Vibration, 260*(5), 867–888. https://doi.org/10.1016/S0022-460X(02)00934-3.

Wong, J. Y. (2001). *Theory of ground vehicles*. NY: Wiley.

Zhang, Y., Chen, W., Chen, L., & Shangguan, W. (2007). Non-stationary random vibration analysis of vehicle with fractional damping. In *Proceedings - 13th national conference on mechanisms and machines (NaCoMM07)* (pp. 171–178). Bangalore.

Zhu, Q., & Ishitobi, M. (2006). Chaotic vibration of a nonlinear full-vehicle model. *International Journal of Solids and Structures, 43*(3–4), 747–759. https://doi.org/10.1016/j.ijsolstr.2005.06.070.

Submit your manuscript to a SpringerOpen journal and benefit from:

- ► Convenient online submission
- ► Rigorous peer review
- ► Open access: articles freely available online
- ► High visibility within the field
- ► Retaining the copyright to your article

Submit your next manuscript at ► springeropen.com